Line Shapes of Paramagnetic Resonances of Chromium in Ruby*†

W. J. C. GRANT‡ AND M. W. P. STRANDBERG

*Research Laboratory of Electronics and Department of Physics, Massachusetts Institute of Technology,
Cambridge, Massachusetts*

(Received 20 January 1964)

Using the formalism of the preceding paper, detailed numerical calculations are performed for the line shapes of paramagnetic resonances of chromium in ruby. Not only half-widths and intensities, but the fine details of the line shapes are accounted for, over a concentration range of about 0.01% to 1%. In particular it is found that (1) the dipolar line departs only slightly from the Lorentzian at the highest attainable concentrations, (2) the line is predominantly nondipolar at low concentrations, (3) no inference is possible from moments as to the magnitude or parametric behavior of intensities and half-widths, (4) neither exchange nor clustering of impurities affect the line shape at low concentrations, (5) exchange cannot narrow the $(\frac{1}{2},-\frac{1}{2})$ transition. Various explanations for the observed residual width at vanishing concentrations are discussed in the light of these findings.

I. INTRODUCTION

IN this paper we analyze the line shapes of the microwave transitions of Cr^{3+} in ruby, in terms of the statistical theory of spin-spin interactions which we have previously developed.[1] Ruby gives considerable scope to the application of the theory, because, in addition to Cr-Cr dipole interaction, strong and fairly long-range exchange interaction is known to be present,[2] as well as interactions with the paramagnetic aluminum nuclei. Furthermore, the line shapes and intensities have been extensively studied experimentally, and have resisted interpretation on the basis of moments.[3]

Following our previous method, we first solve the two-body problem in Sec. II. We can then immediately calculate as many moments as we please, and we illustrate the procedure in Sec. III. In Sec. IV we calculate the line shapes in detail. In Sec. V we consider more specifically the effects of near-neighbor interactions, both dipolar and exchange. Finally, in Sec. VI, we offer some comments on the "residual" width, that is, the line shape that one obtains in the limit of vanishing concentrations.

II. THE TWO-BODY PROBLEM

The pair Hamiltonian is

$$\mathcal{H} = g\beta \mathbf{H} \cdot (\mathbf{S}_1 + \mathbf{S}_2) - D(S_{z1}^2 + S_{z2}^2 - \tfrac{1}{3}S_1^2 - \tfrac{1}{3}S_2^2)$$

$$+ J_{\text{exch}}\mathbf{S}_1 \cdot \mathbf{S}_2 + \frac{g^2\beta^2}{r^3}\left[\mathbf{S}_1 \cdot \mathbf{S}_2 - 3\frac{(\mathbf{r} \cdot \mathbf{S}_1)(\mathbf{r} \cdot \mathbf{S}_2)}{r^2}\right]. \quad (1)$$

The terms have the same meaning as the corresponding terms of Eq. (1) in Ref. 1. The g value is $g_{\parallel} = 1.9840$, $g_{\perp} = 1.9867$.[4,5] The crystal field parameter D has the value 5.75 kMc/sec.[6] The energy levels of the corresponding single-particle Hamiltonian have been derived in detail by Davis and Strandberg[7] and by Schulz-DuBois.[8]

We choose the crystal axis as the quantization axis. To avoid the necessity of numerical diagonalization at this early stage, we take $\mathbf{H} = H_z$.

When $J_{\text{exch}} > D$, we use a representation in which $\mathbf{S}_1 \cdot \mathbf{S}_2$ is diagonal, with wave functions and matrix elements defined in Eqs. (2) and (3) of Ref. 1. The zeroth-order pair matrix consists of four diagonal blocks, corresponding to $\mathbf{J} = \mathbf{S}_1 + \mathbf{S}_2 = 3, 2, 1, 0$. The off-diagonal crystal field terms connect only states differing by several multiples of J_{exch}. We treat both the crystal field and the dipole interaction in first order. In this coupled scheme, some of the allowed transitions have frequencies which in first order coincide with those of the main ruby line. Specifically, for $\mathbf{J} = 3$ and $M = 3 \rightarrow M = 2, \Delta E = g\beta H - 2D$; for $J = 3$ and $M = -2 \rightarrow M = -3$, $\Delta E = g\beta H + 2D$; for $J = 2$, all transitions have $\Delta E = g\beta H$. In Table I, we list these transitions according to the following notation: Transition probability$=g$; first-order dipole perturbation$= q \cdot g^2\beta^2(3 \cos^2\theta - 1)/r^3$.

When $J_{\text{exch}} < D$, the representation is defined by Eqs. (5) and (6) of Ref. 1, in which the crystal term is diagonal, and in which the pair matrix breaks up into completely unconnected blocks of even and odd linear combinations of single-particle states. All allowed

¹ W. J. C. Grant and M. W. P. Strandberg, preceding paper, Phys. Rev. 135, A715 (1964).

² L. Rimai, H. Statz, M. J. Weber, G. A. de Mars, and G. F. Koster, Phys. Rev. Letters 4, 125 (1960); H. Statz, L. Rimai, M. J. Weber, G. A. de Mars, and G. F. Koster, J. Appl. Phys. 32, 2185 (1961); M. J. Weber, L. Rimai, H. Statz, and G. A. de Mars, Bull. Am. Phys. Soc. 6, 141 (1961).

³ A. A. Manenkov and A. M. Prokhorov, Zh. Eksperim. i Teor. Fiz. 38, 1042 (1960) [English transl.: Soviet Phys.—JETP 11, 751 (1960)].

⁴ A. A. Manenkov and A. M. Prokhorov, Zh. Eksperim. i Teor. Fiz. 28, 762 (1955) [English transl.: Soviet Phys.—JETP 1, 611 (1955)].

⁵ M. Zaripov and I. Shamonin, Zh. Eksperim. i Teor. Fiz. 30, 291 (1956) [English transl.: Soviet Phys.—JETP 30, 291 (1956)].

⁶ J. E. Geusic, Phys. Rev. 102, 1252 (1956).

⁷ C. F. Davis, Jr., and M. W. P. Strandberg, Phys. Rev. 105, 447 (1957).

⁸ E. O. Schulz-DuBois, Bell System Tech. J. 38, 271 (1959).

TABLE I. Pair transitions (coupled scheme).

$\Delta E = g\beta H + 2D$		$\Delta E = g\beta H$		$\Delta E = g\beta H - 2D$	
g	q	g	q	g	q
3/2	9/4	1	−9/4	3/2	−9/4
		3/2	−3/4		
		3/2	3/4		
		1	9/4		

TABLE III. Moments for ruby lines, $n = 0.1\%$.

m	a_m	$(\frac{1}{2}, -\frac{1}{2})$ V_m'	$\langle\omega^m\rangle^{1/m}$	$(\frac{3}{2},\frac{1}{2})$ V_m'	$\langle\omega^m\rangle^{1/m}$
2	−0.6	0.509×10^8	225.2	0.433×10^{18}	208
3	−0.0571425	0	0	0.299×10^{11}	284
4	−0.0285725	0.648×10^{15}	897	0.599×10^{15}	880
5	−0.0051940834	0	0	0.2016×10^{19}	1150
6	−0.001412215	0.2555×10^{23}	1716	0.2455×10^{23}	1699

transitions now have frequencies corresponding to some single-particle transition. In Table II, we tabulate these transitions, according to the notation: Transition probability $= g$, first-order dipole perturbation $= q \cdot g^2\beta^2(3\cos^2\theta - 1)/r^3$, first-order exchange perturbation $= t \cdot J_{\text{exch}}$. We notice that 6 pair transitions are clustered around each of the single-particle transitions.

The complete Hamiltonian matrices, as well as a tabulation of the dipole perturbations for the first 16 neighbor shells, can be found in Ref. 9.

III. MOMENTS

Moments of any order are immediately accessible once the q's and g's of the two-body problem are known. They are given by Eqs. (47), (67), and (64) of Ref. 1. We recall [Eq. (47)] that the moments $\langle\omega^m\rangle$ have leading terms $-nV_m'$, where n is the molar spin concentration and, according to Eqs. (67) and (64) of Ref. 1,

$$V_m' = (8\pi/9x_0v)m!a_m(g^2\beta^2x_0/\hbar)^m \sum_j g_jq_j^m / \sum_j g_j, \qquad (2)$$

$$a_m = \left[\frac{2^{m-1}}{m!} + \frac{1}{m!}\sum_{k=0}^{m}(-)^{m-k}\binom{m}{k}\right.$$
$$\left.\times\left(3^k - k\sum_{p=0}^{k}\frac{3p}{p+\frac{1}{2}}\right)\right]. \qquad (3)$$

The quantity $x_0^{-1/3} \equiv r_0 =$ effective nearest-neighbor distance, v is the average volume per lattice site, and $\binom{m}{k}$ denotes a binomial coefficient. The j sum runs over those pair transitions which have a common transition frequency if one neglects the dipole perturbation. In

TABLE II. Pair transitions (uncoupled scheme).

$\Delta E = g\beta H - 2D$			$\Delta E = g\beta H$			$\Delta E = g\beta H + 2D$		
g	q	t	g	q	t	g	q	t
3/2	−9/4	0	1	−3/4	3	3/2	9/4	0
3/4	3/2	−3/2	1	3/4	−3	3/4	−3/2	3/2
3/2	1/4	2	2	−3/2	−3/2	3/2	−1/4	−2
3/4	−1/2	−5/2	2	3/2	3/2	3/4	1/2	5/2
3/4	3/2	−3/2	1	−9/4	0	3/4	−3/2	3/2
3/4	3/2	3/2	1	9/4	0	3/4	−3/2	−3/2

W. J. C. Grant, Ph.D. thesis, Department of Physics, MIT, Cambridge, Massachusetts, May 1962 (unpublished).

Table III, we tabulate a_m, V_m', and $\langle\omega^m\rangle^{1/m}$ up to $m = 6$, for the $(\frac{1}{2}, -\frac{1}{2})$ and $(\frac{3}{2},\frac{1}{2})$ transitions. We take $x_0 = 0.048988$ Å^{-3}, or $r_0 = 2.73$ Å. The concentration is taken as 0.1%. For other concentrations n, the moments can be obtained to first order in n by multiplying the tabulated values by $(0.001/n)^{1/m}$. The $\langle\omega^m\rangle^{1/m}$ are given in megacycles.

We notice that the moment series shows no sign of convergence, at least, as far as the sixth moment. A construction of the line from its moments is clearly impractical in this case. We also note the existence of odd moments for the $(\frac{3}{2},\frac{1}{2})$ transition.

It is of some interest to compare our moments with those obtained by the usual methods. According to Van Vleck,[10] the second moment is given by

$$\langle\omega^2\rangle = n(g^4\beta^4/\hbar^2)\sum_k r_{jk}^{-6}(3\cos^2\theta_{jk} - 1)^2\alpha, \qquad (4)$$

where $\alpha = 81/32$ for the $(\frac{1}{2}, -\frac{1}{2})$ transition and $69/32$ for the $(\frac{3}{2},\frac{1}{2})$ transition.[3] If we replace the lattice sum by an integral from r_0 to ∞, Eq. (4) becomes

$$\langle\omega^2\rangle = n(16\pi x_0/15v)(g^4\beta^4/\hbar^2)\alpha. \qquad (5)$$

This is to be compared with Eq. (68) of Ref. 1.

$$\langle\omega^2\rangle = n(16\pi x_0/15v)(g^4\beta^4/\hbar^2)\sum_j g_jq_j^2 / \sum_j g_j. \qquad (6)$$

Using the g_j and q_j of Table II, we obtain for the ratio of the j sums the values 81/32 and 69/32, in exact
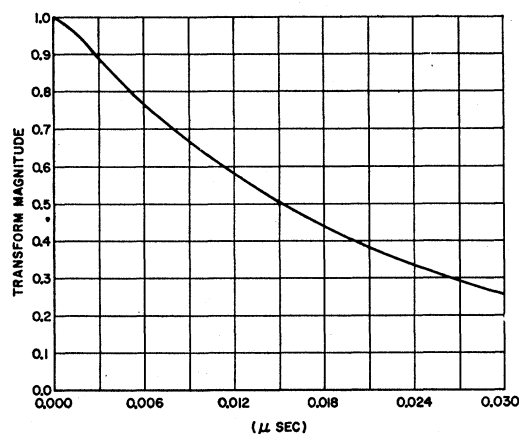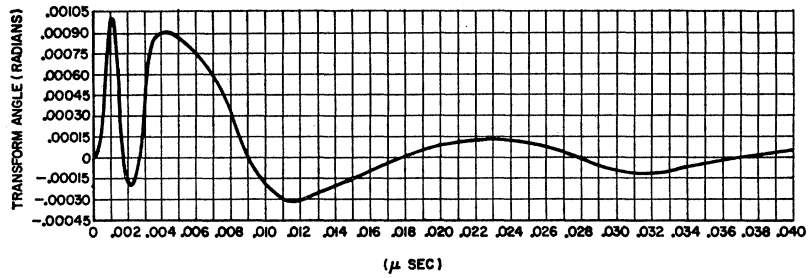

FIG. 1. Fourier transform (magnitude).

[10] J. H. Van Vleck, Phys. Rev. 74, 1168 (1948).

FIG. 2. Fourier transform (angle).

agreement with the results derived by Manenkov and Prokhorov.

We have not investigated the coincidence of our method and Van Vleck's for higher moments.

IV. CALCULATION OF THE LINE SHAPE

The physical line shape is a composite effect of the mutual interaction of the Cr^{3+} ions through dipole fields and through exchange forces and of their interaction with ions in the host lattice. From a computational point of view, we can think of two contributions to the Cr-Cr interactions—one from near neighbors whose positions must be taken into account exactly, and one from distant neighbors whose positions can be approximated by a continuous distribution. We first discuss the line shape derived on the basis of Cr-Cr dipole interaction only, assuming a continuous dipole distribution with inner cutoff radius r_0. Then we amalgamate the "inhomogeneous" portion of the line, arising from interactions with the host lattice. Finally, we take into account the contribution, both dipolar and exchange, from those neighbors which must be handled by a discrete sum.

From Ref. 1, the line shape $I(\omega)$ is the Fourier transform of the relaxation function $\exp(-nV')$, where

$$V'(\rho) = \text{lattice sum} + \sum_j g_j V_j(\rho) / v \sum_j g_j. \qquad (7)$$

The j sum has the same significance as in Eq. (2), and the V_j can be conveniently calculated from expansions given in part I, Eqs. (62)–(64). V' will, in general, be complex, with a symmetric real part and an antisymmetric imaginary part. For the first step of the computation, we omit the lattice sum in Eq. (7). In Figs. 1 and 2, we show the magnitude and angle of the complex transform, calculated for the $(\frac{3}{2}, \frac{1}{2})$ transition, a concentration $n = 0.05\%$, and $r_0 = 6.3$ Å. The magnitude of the transform is almost an exponential of the form $\exp(-a|\rho|)$, with its cusp at the origin rounded into a Gaussian peak. The nonvanishing angle is directly connected with the nonvanishing odd moments, that is, with an asymmetry in the line. We notice, however, that the angle is very small and consists essentially of a few rapid wiggles near the origin. In frequency space, this implies a small effect, occurring in the wings of the line. The odd moments, proportional to the odd

derivatives at the origin in ρ space, are large; the asymmetry in ω space, though heavily weighting the moments because it occurs in the far wings, will for that very reason be scarcely observable.

The results of inverting transforms such as shown in Figs. 1 and 2 are summarized in Figs. 3–7.
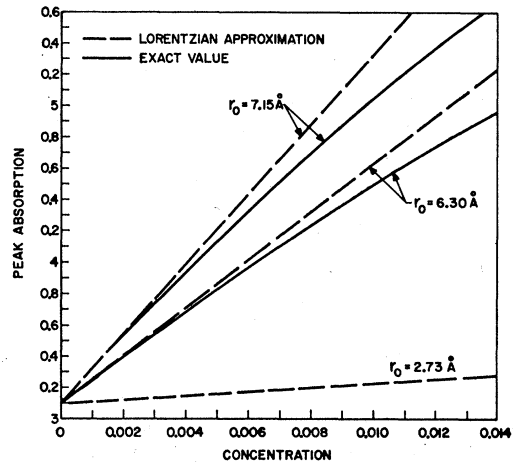
FIG. 3. Continuous distribution—$(\frac{1}{2}, -\frac{1}{2})$ transition—peak absorption (arbitrary units) versus concentration (mole fraction).
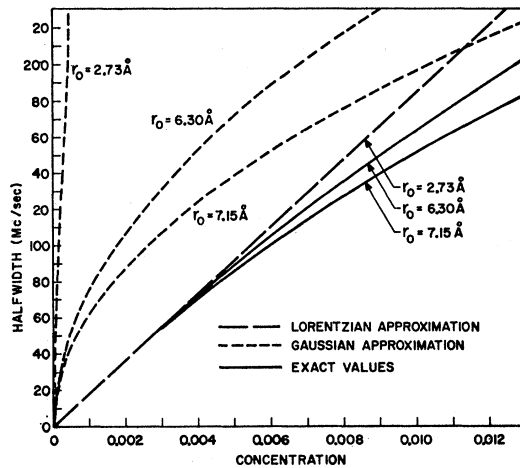
FIG. 4. Continuous distribution—$(\frac{1}{2}, -\frac{1}{2})$ transition—half-width (Mc/sec) versus concentration (mole fraction).
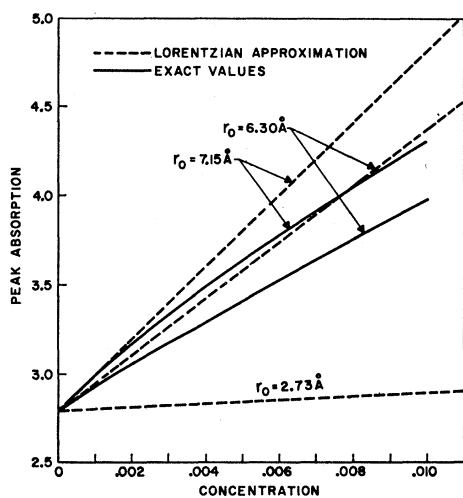
FIG. 5. Continuous distribution—$(\frac{3}{2},\frac{1}{2})$ transition—peak absorption (arbitrary units) versus concentration (mole fraction).

In the previous paper[1] we discussed limiting line shapes, and we pointed out that for small n and small r_0, the shape must be Lorentzian, whereas for large n and large r_0 it must be Gaussian. In the Lorentzian limit,

$$\text{half-width} = C_1 n, \tag{8}$$

$$\text{peak intensity} = C_2 + C_3 n r_0^3. \tag{9}$$

In the Gaussian limit,

$$\text{half-width} = C_4 n^{1/2} r_0^{-3/2}, \tag{10}$$

$$\text{peak intensity} = C_5 n^{1/2} r_0^{3/2}. \tag{11}$$

The constants C_1 through C_5 depend on the crystal structure and on the transition under consideration, as indicated in Eqs. (59)–(72) of Ref. 1. In our figures we indicate these limiting forms, together with the exact calculated behavior. On Figs. 3 and 4, we show the
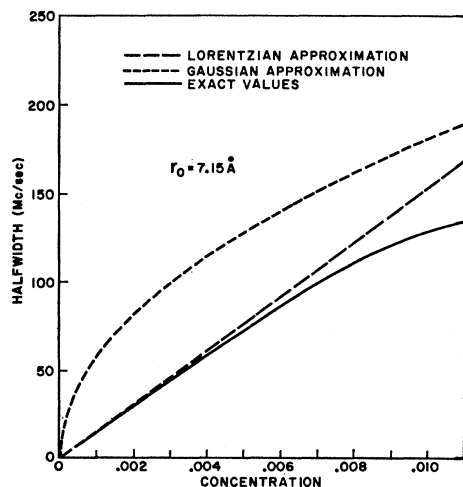

FIG. 6. Continuous distribution—$(\frac{3}{2},\frac{1}{2})$ transition—half-width (Mc/sec) versus concentration (mole fraction).

dependence of intensity and half-width on concentration for the $(\frac{1}{2}, -\frac{1}{2})$ transition. The exact calculated values for $r_0 = 2.73$ cannot be distinguished, on the scale of our graph, from the Lorentzian limit. Figures 5 and 6 pertain to the $(\frac{3}{2},\frac{1}{2})$ transition. In Fig. 6 we show results for one r_0 only. In Fig. 7, we show the dependence of the half-width on r_0. Although the Gaussian approximation and the actual behavior are wildly different in the region of interest, one can begin to see that they would asymptotically approach one another for very large r_0.

It is clear that in dilute crystals, the dipole interaction gives rise to line shapes of which neither the actual magnitudes nor the parametric dependences can be related to the second moment in any simple fashion.

The second step in the computation involves interactions between the Cr spins and other species in the host lattice. Such interactions are, at least to first order, independent of Cr-Cr interactions. In general, the joint effect of any number of statistically independent interactions is obtained by convoluting the separate effects. This well-known statistical theorem[11] underlies the terminology of "inhomogeneous" broadening introduced into the present context by Portis.[12] Interactions with neighboring aluminum nuclei, for instance, evidently fulfill the independence criterion to an excellent approximation, for small Cr concentrations. The contribution of such interactions can be isolated experimentally as the residual line shape in the limit of vanishing Cr concentration. This residual shape is a Gaussian of half-width 17.8 Mc/sec. We discuss the origin of the residual line in Sec. VI. For now, we point out that 18 Mc/sec corresponds to the dipolar width at about 0.1% concentration, almost independent of
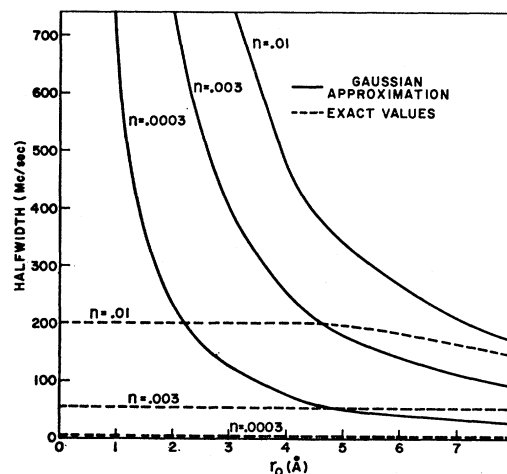

FIG. 7. Continuous distribution—$(\frac{1}{2}, -\frac{1}{2})$ transition— half-width (Mc/sec) versus $r_0(\text{Å})$.

[11] W. Feller, *An Introduction to Probability Theory and Its Applications* (John Wiley & Sons, Inc., New York, 1957), Chap. 11 and Chap. 12.
[12] A. M. Portis, Phys. Rev. **91**, 1071 (1953).

the value assumed for r_0 (see Fig. 4). This means that Cr self-broadening makes a very small contribution to the total line in "pink" rubies, and becomes predominant only in very dark rubies. Consequently, relations (8) and (9) do not apply to actually observed lines. Instead, for concentrations of the order of 0.01% one expects

$$\text{half-width} \approx \text{constant} \approx 17.8 \text{ Mc/sec} \quad (12)$$

$$\text{intensity} \propto n. \quad (13)$$

These relations are, in fact, experimentally verified. We notice that, whether the Gaussian broadening is present or not, the actual widths and intensities will not show the $n^{1/2}$ dependence of the Gaussian approximation. The relations are always asymptotically linear.

We also can now see why observed line shapes go from Gaussian to Lorentzian with increasing concentration. The dipolar line itself is almost pure Lorentzian at low concentrations, and begins to tend towards the Gaussian shape at very high ones. Because of the "inhomogeneous" Gaussian contribution, however, this trend is at first reversed. The resulting oscillation between the two shapes is illustrated in Fig. 8 in terms of the relationship between the absorption width and the width of its derivative. The points shown are experimental ones. (See Appendix A.)

The third step of the computation incorporates the lattice sum in Eq. (7) for near lying sites. Some, but not necessarily all, the spins situated at these sites will be exchange coupled to the reference spin. According to Eq. (29) of Ref. 1,

$$V'_{\text{lattice sum}} = \frac{1}{\sum_u g_u} \sum_c \sum_{r_i < r_1} p_i g_c \{1 - \exp[i\rho\omega(\mathbf{r}_i, q_c)]\}$$

$$+ \sum_u \sum_{r_1 < r_i < r_0} p_i g_u \{1 - \exp[i\rho\omega(\mathbf{r}_i, q_u)]\} . \quad (14)$$

The subscripts c and u refer to the coupled and uncoupled representations which specify the g's and q's (Tables I and II) for large and small exchange, respectively. Exchange is assumed large for $r < r_1$, negligible for $r > r_1$. The lattice sum cuts off at r_0. The "clustering factor" p_i is defined as the ratio of the actual probability that site i is occupied to the probability of occupation if the distribution were random.

Abbreviating the notation by using α as an over-all index, we obtain the transform of the lattice sum as follows:

$$\int_{-\infty}^{\infty} d\rho e^{-i\omega\rho} \exp[-n \sum_\alpha p_\alpha g_\alpha (1 - e^{i\omega\alpha\rho})/\sum_j g_j]$$

$$\approx \exp(-n \sum_\alpha p_\alpha g_\alpha/\sum_j g_j)$$

$$\times \int_{-\infty}^{\infty} d\rho e^{-i\omega\rho}[1 + (n/\sum_j g_j) \sum_\alpha p_\alpha g_\alpha e^{i\omega\alpha\rho}] \quad (15)$$
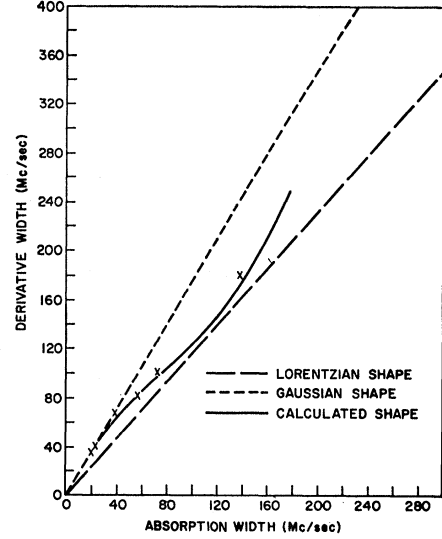

FIG. 8. Absorption half-width (Mc/sec) versus p-p derivative width (Mc/sec).

$$= \exp(-n \sum_\alpha p_\alpha g_\alpha/\sum_j g_j)$$

$$\times [\delta(\omega) + (n/\sum_j g_j) \sum_\alpha p_\alpha g_\alpha \delta(\omega - \omega_\alpha)]. \quad (16)$$

Here, δ represents the delta function. The neglect of higher powers of n in the expansion of Eq. (15) introduces only small errors for physically significant concentrations.

Since the continuous distribution and the lattice sum appear as products in ρ space, the joint contribution in ω space is obtained by convolution. In this sense, (16) embodies the satellite spectrum, and gives a simple prescription for joining it to the main line. We notice that the line shapes of the satellites and of the main transitions are interdependent. The possibility of clustering can be taken into account at this point by varying the p_α. Our numerical calculations all assume that the p_α are equal, though not necessarily equal to unity.

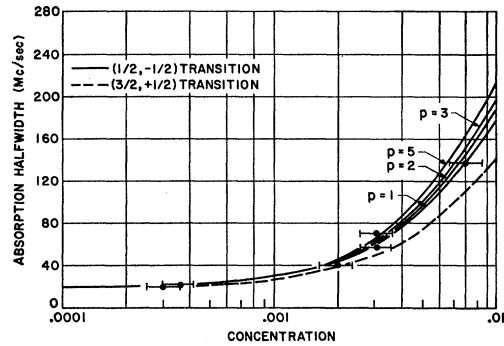We exhibit in Figs. 9–12 the behavior of various line

FIG. 9. Absorption half-width (Mc/sec) versus concentration (mole fraction).
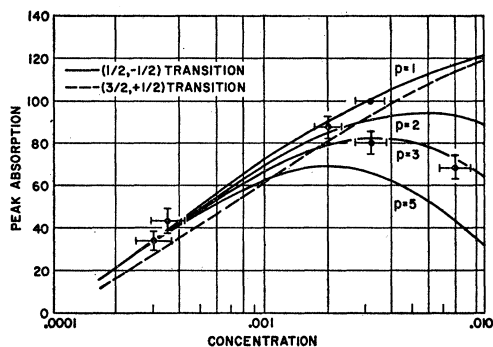
FIG. 10. Peak absorption (arbitrary units) versus
concentration (mole fraction).

FIG. 12. Peak-peak derivative height (arbitrary units)
versus concentration (mole fraction).

shape parameters, calculated this time for the entire composite line. Strong exchange has been assumed as far as 7.15 Å, which represents an upper limit to the exchange radius. The discrete sum has been carried to the same distance, with a continuous dipole density then extending to infinity. The points shown are experimental ones and apply to the $(\frac{1}{2}, -\frac{1}{2})$ transition. We have assigned concentrations, not on the basis of our study of line shapes, since this would involve a circularity in the argument, but on the basis of chemical analyses. We note that the points for two of the high-concentration crystals fall consistently on curves with large p values.

The four parameters whose concentration dependence we show in Figs. 9–12 obviously do not exhaust the line shape. To illustrate the type of agreement we obtain between calculation and experiment, we present in Fig. 13 an experimentally derived line shape against a background of theoretical line shapes bracketing the appropriate concentration. We stress that, as the concentration changes, the curves do not merely change scale, but undergo complicated changes in shape. This fact can be accentuated by using the derivative of the absorption and scaling the curves to identical peak-to-peak values. We show such a set of curves in Fig. 14.

We now revert to the question of asymmetry in the $(\frac{3}{2},\frac{1}{2})$ line. In Table IV, we summarize calculations for
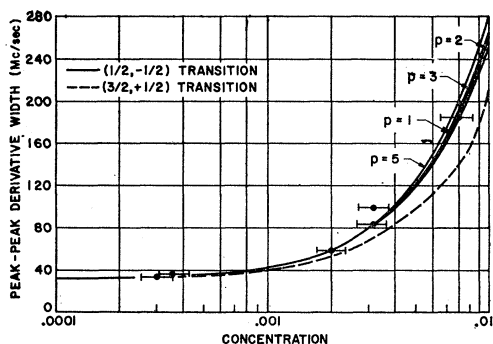
four concentrations to show the nature and extent of the expected asymmetry. The calculations were made under the same assumptions as those of Figs. 9–12, with $p=1$. We quote intensities for roughly the following multiples of the half-widths: 0, 1, 2, 5. Intensities are given in arbitrary but consistent units; frequencies are in mc. It is obvious at a glance that it would be hopeless to see the asymmetry in a resonance experiment. Conceivably it might be detectable in a cross-relaxation experiment.

V. NEAR-NEIGHBOR EFFECTS

One of the striking features of Figs. 9–12 is the ineffectuality of the near neighbors at low concentrations. The different p curves, for all the line shape parameters, merge for concentrations less than 0.05%. The relative unimportance of the near neighbors in dilute crystals can be understood from three considerations: (1) The contribution of these neighbors to the absorption goes like n^2. Intuitively, the number of pairs in a fixed region is proportional to n^2; more formally, Eq. (16) shows that the near-neighbor perturbation scales by a factor n a line whose area is already proportional to n. (2) While the near neighbors produce the largest single perturbations, the number of neighbors increases faster with distance than their individual perturbation decreases. (In Ref. 1, we met this phenomenon as a logarithmic divergence.) (3) The very largeness of

FIG. 11. Peak-peak derivative width (Mc/sec) versus
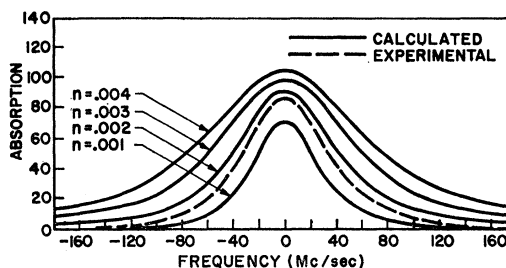concentration (mole fraction).

FIG. 13. Calculated and experimental absorptions (arbitrary
units) versus frequency (Mc/sec), for sample 3.

their individual perturbations make their effect relevant principally to the far wings of the line.

As a consequence, for low concentrations, it makes no difference what one assumes about the near neighbors. Whether they are clustered or not, exchange coupled or not, considered as point dipoles or smeared into a continuous distribution—none of this will significantly affect the observable central part of the line. We note, however, that the reverse is true of the moments. These quantities weight most heavily the far wings of the line, where the near neighbors produce a relatively large effect. If we ignore all the atoms outside a radius of, say 7.15 Å, we pick up about 90% of the second moment; if we ignore all the atoms inside this same radius, we may pick up 90%, or more, of the line area.

For concentrations higher than about 0.1%, the near neighbor contribution becomes significant, certainly as far as intensities are concerned. The effect of the near neighbors is to take power out of the central portion of the line and spread it more or less uniformly into the
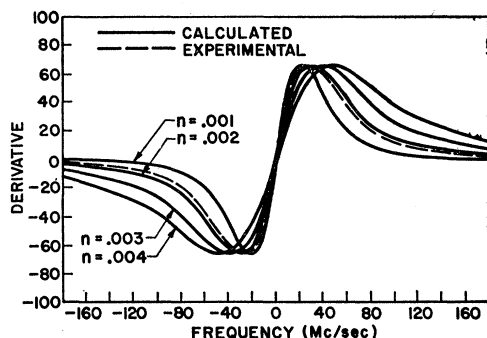

FIG. 14. Scaled calculated and experimental derivatives (arbitrary units) versus frequency (Mc/sec) for sample 3.

wings. More formally, the near neighbors can alter considerably the exponential coefficient in Eq. (16), while affecting only slightly the line shape as a whole. Thus, the center intensity depends on the near neighbors exponentially while the compensation in area is spread over the whole spectrum. An actual decrease in intensity at higher concentrations has been observed both by us and by Manenkov and Prokhorov.[3] Our theory accounts for this phenomenon very naturally as an effect of clustering. We see from Figs. 9–12 that our crystal with $n=0.8\%$ shows significant clustering effects, as does one of the crystals with $=0.3\%$. In contrast, the other crystal with $n=0.3\%$ was a high-quality slow grown annealed crystal, and shows no significant evidence of clustering. The correlation between the quality of a crystal and the p values assignable to its line shape characteristics is a very interesting and useful confirmation of our calculations.

The observed decrease in intensity cannot be accounted for, at least for the $(\frac{1}{2}, -\frac{1}{2})$ transition, by

TABLE IV. Asymmetry in the $(\frac{3}{2},\frac{1}{2})$ transition.

$n=0.0003$				
frequency	0	21	39	102
$I(\omega)$	0.8530	0.4075	0.08742	0.00515
$I(-\omega)$	0.8530	0.4071	0.08677	0.00550
$n=0.001$				
frequency	0	28	53	121
$I(\omega)$	1.9200	0.9107	0.2752	0.03338
$I(-\omega)$	1.9200	0.9061	0.2715	0.03311
$n=0.010$				
frequency	0	125	275	660
$I(\omega)$	3.735	2.054	0.5960	0.04729
$I(-\omega)$	3.735	1.973	0.4818	0.08265

exchange. As we shall now show, exchange can have only a minuscule effect on the line shape of this transition.

As we have pointed out previously,[1] exchange causes detailed and specific changes in the energy structure. These changes cannot in this case be adequately accounted for by replacing them with an averaged correlation effect, or by invoking the 10/3 factor[13] in blanket fashion. In the present case, the $J=2$ manifold in the coupled scheme contributes very nearly as much to the $(\frac{1}{2}, -\frac{1}{2})$ transition as would have been contributed in the uncoupled scheme. In Table V, we compare the results derived from considering exchange large or small, for neighbor shells 8–16. The differences are negligible. Despite the existence of strong exchange, this line is in no sense exchange narrowed.

Exchange narrowing does occur for the $(\frac{3}{2},\frac{1}{2})$ transition. The reason is that the coupled scheme contributes very little to this transition, compared with the uncoupled scheme. Nevertheless, for this line too, the modification of the observed line shape by exchange is negligible at low concentrations. The parameters for exchange narrowing are derived by reference to moments, and the half-width is not related to moments in dilute systems. Exchange affects the extreme wings of the line, altering the moments without altering appreciably the shape of the central hump.

VI. THE RESIDUAL WIDTH

We now consider the problem of the residual width of 18 Mc/sec. We shall first consider various explana-

TABLE V. Effect of exchange on the $(\frac{1}{2}, -\frac{1}{2})$ transition.

Concentration (%)	Absorption peak		Absorption half-width (Mc/sec)	
	$J=\infty$	$J=0$	$J=\infty$	$J=0$
0.02	24.8	25.4	19.8	19.8
0.04	42.4	43.2	22.0	22.0
0.1	71.9	72.9	29.5	29.6
0.2	91.3	92.0	44.1	44.4
0.4	105	105	76.3	76.8
0.9	119	114	151	153

[13] P. W. Anderson and P. R. Weiss, Rev. Mod. Phys. 25, 269 (1953).

tions that have been offered for this phenomenon, and then propose an alternative explanation of our own.

Perhaps the most widely used scapegoat for unexplained line shape phenomena is the crystal field. We can rule out the crystal field, however, because the crystal field does not appear in the transition energy of the $(\frac{1}{2}, -\frac{1}{2})$ transition. Furthermore, $\partial f/\partial \theta = 0$ at our $0°$ orientation, so that small angular variations in the crystal field cannot affect the $(\frac{3}{2}, \frac{1}{2})$ transition either. The two transitions do in fact approach, within experimental error, the same limiting linewidth. One could argue that the crystal field also affects the g value, and that slight variations in this factor might produce noticeable effects at fields of a few thousand gauss. These variations would be field-dependent, however, and the residual width is the same for transitions at 840, 3300, and 7400 G. We can show how completely impossible this supposition is by a very simple calculation. If we believe the crystal field approximation, the spin Hamiltonian, with $\mathbf{H} = H_z$, can be written[14]

$$\mathcal{3C} = 2.002(1-\lambda\Lambda)\beta H S_z - \lambda^2 \Lambda S_z{}^2, \qquad (17)$$

where λ is the spin-orbit coupling constant, and Λ is a second-order sum over higher orbital states. We identify $g = 2.002(1-\lambda\Lambda)$ and $D = \lambda^2\Lambda$. A fractional variation of α in the crystal field will cause Λ to go into $\Lambda(1\mp\alpha)$. Consequently, g goes into $[2.002-0.018(1\mp\alpha)]$ and $2D$ goes into $11.5(1\mp\alpha)$ kMc/sec. The numbers are such as to match the experimental ones for $\alpha = 0$. The energy spread due to Δg will be $(0.018\times 1.4H)\alpha$ Mc/sec; that due to $\Delta(2D)$ will be 11.5α kMc/sec. If $H = 3300$ G, the broadening effect of the crystal field via the D term will be 160 times as great as via the g factor. If we ascribe a residual 18 Mc/sec to the g factor, then the $(\frac{3}{2}, \frac{1}{2})$ transition should be broader than the $(\frac{1}{2}, -\frac{1}{2})$ transition by 3 kMc/sec.

We cannot ascribe the residual width to clustering. This explanation originates in the fact that clustering will enhance the second moment, and consequently will broaden the line. As we have seen at length, this argument is a *nonsequitur*. The enhancement of the second moment is produced by slightly enhancing the far wings at a slight expense of intensity in the main line. The line shape of the central hump is changed very little. At low concentrations, the effect of clustering vanishes for all practical purposes.

Macroscopic clustering, that is, macroscopic compared to lattice dimensions, may contribute to the residual width, but cannot be the total cause. Such inhomogeneities raise the effective concentration and reduce the effective crystal volume, giving a broader and less intense line. The line produced, however, would be (almost) Lorentzian, while what is observed is practically pure Gaussian. To keep the shape Gaussian, the dipolar contribution must be substantially

less than half, or less than 9 Mc/sec. The chromium "pockets" must then have a concentration less 0.05%. At any rate, at least 10 Mc/sec must still be accounted for otherwise.

We consider the possibility of impurities. The presence of small quantities of other paramagnetic impurities is *a priori* a plausible supposition. In fact, Thorp *et al.*[15] have found 0.04% iron in flame fusion rubies, independent of the chromium concentration. This amount of impurity is of the right order to account for the residual width. For rubies grown from the vapor phase, they find a constant iron concentration of 0.004%. It would have been interesting if they had made measurements of residual width on these two types of specimens. We do not believe that impurities, iron or otherwise, are the explanation, however. An amount of iron, such as observed by Thorp *et al.*, would produce an immense spectrum of its own, which is not generally observed, although Thorp did observe it in his particular specimens. Furthermore, substantially the same residual width has been observed not only by us, but by many other experimenters. It would be difficult to account for the presence of exactly the same impurity content in many different rubies, both natural and synthetic. This difficulty becomes even more severe if the impurities are not simply iron, but a large number of different species. The number would have to be very large for their individual spectra to be unobservable. Yet their combined effect would always have to give rise to the same linewidth. Furthermore, the same residual width is found in rubies whose chemical content is analytically controlled and verified. Furthermore, the line shape due to impurities in trace amounts must be Lorentzian; what is observed is clearly a Gaussian shape. Furthermore, paramagnetic impurities would clearly affect the static susceptibility. The work of Daunt and others[16-21] shows that the susceptibility can be matched to the chromium four-level system from room temperature to $0.3°K$, over a chromium concentration range from 0.047% to 1.4%. We note that an impurity content of 0.04% would change the susceptibility by a factor of 2 in the lowest concentration studied by Daunt, even if we make the unbelievably unlikely assumption that the partition function of the impurity is the same as that of chromium. (Daunt claims an accuracy of 5%.) While it is doubtless possible to make rubies with an iron or other impurity concentration comparable to the chromium con-

[14] W. Low, in *Solid State Physics*, edited by F. Seitz and D. Turnbull (Academic Press Inc., New York, 1960), Suppl. 2.

[15] J. S. Thorp, J. H. Pace, and D. F. Sampson, British J. Appl. Phys. 12, 705 (1961).

[16] K. Brugger, J. W. Snider, J. G. Daunt, *The Fifth International Conference on Low Temperature Physics*, edited by J. R. Dillinger, University of Wisconsin Press, Madison, Wisconsin, 1958), p. 547.

[17] J. G. Daunt and K. Brugger, Z. Physik. Chem. 16, 203 (1958).

[18] H. L. Davis, Z. Physik. Chem. 16, 213 (1958).

[19] J. G. Daunt, Proc. Phys. Soc. (London) 70, 54 (1957).

[20] J. G. Daunt, D. O. Edwards, M. Dreitman, R. C. Pandorf, and J. W. Snider, *Proceedings of the Seventh International Conference on Low Temperature Physics* (Toronto University Press, Toronto 1960), p. 96.

[21] J. G. Daunt, Bull. Am. Phys. Soc. 1, 116 (1956).

centration, there is no reason to believe such crystals are typical.

We consider spin-lattice interactions. At room temperature these can account for about 1 Mc/sec.[22] Sugihara[23] has proposed a theory of virtual phonon exchange from which he derives a broadening comparable to dipolar broadening. We make two general comments: (1) Sugihara obtains a perturbation comparable to the dipolar one on the basis of interaction with another dipole situated about a lattice dimension away; in other words, he considers the nearest neighbor in a dilute crystal. His interaction falls off as $1/r^3$. But we have already seen that such an interaction, far from rapidly becoming negligible with distance, actually diverges as more neighbors are taken into account. Sugihara's theory leads to an infinite self-energy. Perhaps a renormalization is possible, but it seems to us that so far we have the first term in a diverging series. (2) The virtual phonon exchange is possible only if the two spins have *exactly* the same transition energy. If the line is already broadened, however, the number of spins that fulfill this requirement will be tremendously smaller than the actual number of spins. What is really required is a second-order theory which takes into account the simultaneous interaction with the phonon field and the dipolar field. Only if the excess energy is at the same time absorbed by the dipole field can two spins of even slightly different transition frequencies interact via a virtual process.

Virtual processes, in general, would require a pair of Cr ions, and would therefore give rise to a concentration-dependent process. That such processes make only a small contribution, if any, emerges from the fact that we have already interpreted, with considerable precision, all observed features of the concentration dependence by invoking only known mechanisms.

Hyperfine interaction with the Cr^{53} nucleus (10% natural abundance) certainly exists. Its observation, both in ordinary rubies and in crystals enriched with Cr^{53}, was first reported by Manenkov and Prokhorov.[24] The hyperfine separation is of the order of the residual width. At low-chromium concentrations, the multiplets are resolvable even in unenriched crystals, although their intensity is exceedingly low. This interaction clearly does not help us to solve our present problem.

We now consider magnetic dipole interaction with the aluminum nuclei. We show in Appendix B that this interaction accounts for 5.12 Mc/sec. Since Gaussians add width in rms fashion, subtracting 5.12 from 18 still leaves 17 Mc/sec to be accounted for.

We finally come to our own suggestion for the origin

of the residual width. The existence of covalent bonding in so-called ionic crystals is well known. Low[25] has given convincing arguments for the bonding of iron group ions to neighboring anions in MgO; Tinkham[26] has done the same for ZnF_2. To explain the residual width, we suggest that there may be a slight bonding to the aluminum. This could be either superexchange,[27] via the oxygens, or direct overlap. A slight admixture of aluminum $3s$ wave function would carry with it a contact interaction with the Al nucleus, which could supply the energy perturbation we are looking for. We proceed to calculate, in an admittedly crude and "order of magnitude" fashion, the amount of Al $3s$ wave function we would need. If we write the wave function of a Cr $3d$ electron as

$$\psi = \psi_{Cr} + \epsilon \psi_{Al}, \qquad (18)$$

and if Δ is the hyperfine separation for a $3s$ electron in Al, then the energy resulting from the contact interaction is of the order or $3\epsilon^2\Delta$. (There are three $3d$ electrons in Cr.) The hyperfine separation has been measured for atomic aluminum[28] and is 1450 Mc/sec. Atomic aluminum has one $3p$ electron. If we use the theory of Fermi[29] and Goudsmit,[30] we can obtain the hyperfine separation for one $3s$ electron by an analogy argument. The ratio of the $3s$ separation to the $3p$ separation is given by

$$\Delta(3s)/\Delta(3p) = (8/3)(L+1/2)(J)(J+1) = 3, \quad (19)$$

where, of course, we gloss over corrections for effective charge and shielding. This line of reasoning leads to a value $\epsilon = 0.036$. This number is not obviously unreasonable.

Our hypothesis is attractive because it would also shed light on several other observations. Very narrow electron paramagnetic resonance lines are observed in MgO, where the spectra of the iron group have been exhaustively investigated by Low,[25,31] and in the ThO_2, where the spectrum of Gd has been studied by Shaltiel and Low.[32,33] There is no isotope of Th which has a nuclear moment; Mg^{25} has a small nuclear moment, but its abundance ratio is only 10%. On the other hand, the electron-nuclear double resonance experiments of the Ford group[34–36] leave no doubt that interactions exist between the Cr electrons and the Al nuclei—not

[22] A. A. Manenkov and A. M. Prokhorov, Zh. Eksperim. i Teor. Fiz. 38, 729 (1960) [English transl.: Soviet Phys.—JETP 11, 527 (1960)].
[23] K. Sugihara, J. Phys. Soc. Japan 14, 1231 (1959).
[24] A. A. Manenkov and A. M. Prokhorov, Zh. Eksperim. i Teor. Fiz. 31, 346 (1956) [English transl.: Soviet Phys.—JETP 4, 228 (1957)].

[25] W. Low. Ann. N. Y. Acad. Sci. 72, 69 (1958).
[26] M. Tinkham, Proc. Roy. Soc. (London) A236, 535, 549 (1956).
[27] P. W. Anderson, Phys. Rev. 115, 2 (1959).
[28] H. Lew, Phys. Rev. 76, 1086 (1949).
[29] E. Fermi, Z. Physik 60, 320 (1930).
[30] S. Goudsmit, Phys. Rev. 37, 663 (1931).
[31] W. Low, Phys. Rev. 105, 801 (1957).
[32] D. Shaltiel and W. Low. Phys. Rev. 124, 1062 (1961).
[33] W. Low and D. Shaltiel, Phys. Chem. Solids 6, 315 (1958).
[34] J. Lambe, N. Laurance, E. C. McIrvine, and R. W. Terhune, Phys. Rev. 122, 1161 (1961).
[35] R. W. Terhune, J. Lambe, G. Makhov, and L. G. Cross, Phys. Rev. Letters 4, 234 (1960).
[36] C. Kikuchi, J. Lambe, G. Makhov, and R. W. Terhune, J. Appl. Phys. 30, 1061 (1959).

merely the nearest-neighbor nucleus, but distant nuclei as well. A completely satisfactory explanation of their results has not yet been found. It is possible that an attempt to interpret these experiments in terms of contact interaction, via direct overlap and/or super-exchange, might prove fruitful.

SUMMARY

We have been able to give a detailed account of many of the observed features of the ruby line shapes. We have been able to show clearly the effects of Cr-Cr dipole interaction, exchange, dipole (tensor) interaction with Al^{27}, and the physical disposition of the impurities in the lattice. We have found that careful analysis is needed to interpret the data consistently. A number of general concepts that have passed into the general lore of the subject actually are applicable only asymptotically to special cases, which do not include ruby.

ACKNOWLEDGMENTS

Most of the numerical computations were performed on the IBM-709 computer of the MIT Computation Center. The programs were written by Mrs. B. Grant and one of us (W. G.). We acknowledge the assistance of Mrs. B. Grant, Mrs. G. Hayes, and Mrs. E. Con-nearney in performing the remaining arduous hand calculations.

APPENDIX A: EXPERIMENTAL DATA

Room-temperature measurements of ruby linewidths and intensities as a function of concentration have been published by Manenkov and Prokhorov.[3] We have made measurements covering the same concentration range, for two reasons: (1) Our theory is sensitive not merely to widths but to the details of the line shape. Hence we found it desirable to subject the measured lines to very detailed analysis. (2) The definition of half-width in Ref. 3 seems somewhat uncertain. The definition explicitly given there is the distance from the peak to the half-power point; yet the data quoted are consistent

with data previously given by the same authors[37] if their half-widths are interpreted as peak-to-peak deriva-tive widths. This latter interpretation also makes their data quite consistent with our own.

We used six rubies, all grown by the flame fusion process. Two of these, No. 1 and No. 4 were slow grown annealed crystals. All the crystals were free of macro-scopic inhomogeneities. Small specimens weighing about 15 mg were cut, for study with an X-band cavity spectrometer. Our determination of widths is accurate to within 2%; of relative intensities, to about 10%.

The experimental derivative traces were digitalized and were integrated by means of a computer program. The program allowed automatic corrections for various experimental conditions. It also generated a Gaussian and a Lorentzian to match the peak value and half-width of the experimental absorption. Thus our judg-ment regarding the shape of the line—Gaussian, Lorentz-ian, or intermediate—is not based on the measurement of four points, but of about a hundred. An example of the curves obtained by this procedure is given in Fig. 15. The program integrated the absorption a second time to give the area. We investigated the effect of noise and base-line drift on the results. Half-widths proved quite insensitive, line shapes somewhat sensitive, and areas extremely sensitive. Thus a 2% uncertainty in half-width might typically be associated with a 25% un-certainty in area. For this reason, we feel that concen-tration measurements based exclusively on absorption areas are not very reliable.

The Cr concentration of the crystals was measured by a variety of methods, principally chemical analysis leading to either a spectrographic or colorimetric de-termination. These determinations appear to be re-producible within about 20%. The concentration is, of course, also proportional to the area of the reso-nance line.

In Table VI, we summarize the data. Widths are given in megacycles. Intensities are in arbitrary units, scaled so that the corresponding intensity for the $(\frac{1}{2}, -\frac{1}{2})$ transition of sample No. 4 is 100. Areas are
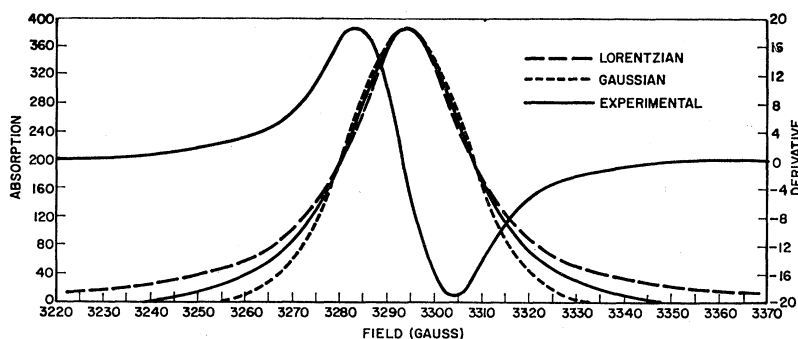

FIG. 15. Experimental absorption and comparison curves (arbitrary units) for sample 3.

[37] A. A. Manenkov and A. M. Prokhorov, Zh. Eksperim. i Teor. Fiz. **31**, 346 (1956) [English transl.: Soviet Phys.—JETP **4**, 288 (1957)].

TABLE VI. Experimental data.

Sample number		1	2	3	4	5	6
Concentration (%)		0.031	0.035	0.20	0.32	0.32	0.79
$(\frac{1}{2}, -\frac{1}{2})$	Deriv. p-p height	96	116	134	100	70	28
	Deriv. p-p width	36.7	38.7	57.3	81.2	100	184
	Absorption peak	34	44	88	100	81	69
	Absorption width	21	22.9	40.1	58.0	71	130
	Area	0.036	0.05	0.19	0.30	0.28	0.56
$(\frac{3}{2},\frac{1}{2})$	Deriv. p-p height	54	62	40	44	23	8
	Deriv. p-p width	37.6	39.8	85.3	91.3	122.5	283
	Absorption peak	18	21	34	45	31	25
	Absorption width	23.4	25.6	57.4	65.8	89.5	203
	Area	0.026	0.031	0.12	0.18	0.17	0.32
$(\frac{3}{2},\frac{1}{2})$ width/$(\frac{1}{2}, -\frac{1}{2})$ width		1.11	1.12	1.43	1.13	1.28	1.56
$(\frac{3}{2},\frac{1}{2})$ area/$(\frac{1}{2}, -\frac{1}{2})$ area		0.72	0.63	0.63	0.60	0.62	0.57

scaled so that the area of the same transition is 0.3. By "width" we mean the half-power half-width.

The ratio of the area for the $(\frac{3}{2},\frac{1}{2})$ transition to that of the $(\frac{1}{2}, -\frac{1}{2})$ transition should be the same as the ratio of the transition probabilities, namely 0.75. In view of the uncertainty in the determination of the areas, the deviations from this number are in themselves not significant. The systematic trend to lower ratios with increasing concentration might be interpreted as an effect of exchange, which, as we have shown, affects the $(\frac{3}{2},\frac{1}{2})$ transition much more than the $(\frac{1}{2}, -\frac{1}{2})$ transition. However, an underestimate of the area becomes more likely with increasing width. This factor would give rise to the same trend, since the excess width of the $(\frac{3}{2},\frac{1}{2})$ transition becomes much more marked at higher concentrations.

This excess width of the $(\frac{3}{2},\frac{1}{2})$ transition is not accounted for by our calculation. The mechanisms included in our calculation predict a narrower, not a broader, line for this transition. We notice that (1) the excess broadening tends to increase with increasing concentration, (2) the annealed crystal No. 4 shows markedly less excess broadening than its conventionally grown neighbors of similar concentration. Both facts can consistently be explained by ascribing the excess width to random variations of the crystal field parameter D, due to internal crystalline strains. Such strains tend to increase with increasing impurity content and are decreased by an annealing process. Since $\partial f/\partial \theta = 0$ at our $0°$ orientation, small variations in the direction of the crystal field will have no effect; what we appear to be seeing are variations in magnitude.

APPENDIX B: DIPOLE INTERACTION WITH ALUMINUM NUCLEI

The contribution of the Cr-Al interaction to the Cr resonance line shape can be calculated in exactly the same fashion as the contribution of the Cr-Cr interaction. A full-scale calculation is unnecessary in this case, however, since the Al concentration is virtually 100%, guaranteeing an almost pure Gaussian line. A second moment calculation will suffice.

In this Appendix, we treat, more generally, the interaction of two different paramagnetic species. Two species are considered different if, in a given magnetic field, none of the transitions of one species overlaps any of the transitions of the other. Our discussion has two parts. First we discuss the particular version of the moment formulation that is applicable in this case; secondly, we calculate the relevant lattice sum for ruby.

(1) Van Vleck's[10] moment method applies directly only to a set of simple Zeeman levels. If there is a zero-field splitting, the theory must be modified, as shown by Abragam and Kambe,[38] Kambe and Usui,[39] and Ishiguro, Kambe, and Usui.[40] Projection operators are then used to single out that portion of the transition operator S_x which connects the particular states under consideration.

One can readily see, however, that the original Van Vleck formulation, unembellished by projection operators, will in all cases give the correct result if the broadening is due to another magnetic species. The dipolar broadening is in general due to two effects. One is the spread of the local magnetic field due to the other dipoles; the other is the simultaneous flipping of two spins, with exchange of energy. The different species cannot contribute to the flipping process, because the transition energies are, by definition, not comparable. But it can contribute to the variations of the magnetic field. It is clearly only the flipping term that is affected by projection operators.

We can put this idea more formally. Consider the Hamiltonian

$$H = H_0 + H', \qquad (B1)$$

where H_0 contains all forms of energy, except that of the dipolar interaction with some other species. This last

[38] A. Abragam and K. Kambe, Phys. Rev. **92**, 894 (1953).
[39] K. Kambe and T. Usui, Progr. Theoret. Phys. (Kyoto) **8**, 302 (1952).
[40] E. Ishiguro, K. Kambe, and T. Usui, Physica **17**, 310 (1951).

interaction is contained in H'.

$$H' = \sum_k C_{jk} S_{zj} S_{zk}, \qquad (B2)$$

$$C_{jk} = (gg'\beta^2/hr_{jk}^3)(3\cos^2\theta_{jk}-1), \qquad (B3)$$

where the jth atom is the one we are considering and the atoms indexed on k are those of the other species. Using the notation $\hat{S}_x$ for the projected Sx_j operator,

$$\langle\omega^2\rangle = -\mathrm{Tr}(H,\hat{S}_x)^2/\mathrm{Tr}(\hat{S}_x)^2. \qquad (B4)$$

Now

$$(H,\hat{S}_x)^2 = [(H_0,\hat{S}_x)+(H',\hat{S}_x)]^2 \qquad (B5)$$

$$= (H_0,\hat{S}_x)^2+(H',\hat{S}_x)^2+[(H_0,\hat{S}_x),(H',\hat{S}_x)]_+. \qquad (B6)$$

The trace of the cross term in (B6) vanishes because $\mathrm{Tr}S_{zk}=0$. The first term in (B6) simply yields $\langle\omega_0^2\rangle$ by definition. The term of interest is the second one. Since $\hat{S}_x$ commutes with S_{zk}, we have essentially a constant time S_{zj}.

$$(KS_{zj},\hat{S}_x) = iK\hat{S}_y. \qquad (B7)$$

Since

$$\mathrm{Tr}(\hat{S}_y)^2 = \mathrm{Tr}(\hat{S}_x)^2, \qquad (B8)$$

the result of the second term is just K^2, or specifically

$$\sum_{kk'} C_{jk}C_{jk'}S_{zk}S_{zk'}. \qquad (B9)$$

We note that the effect of projecting S_x has cancelled out. From this point on, we are coincident with Van Vleck's treatment of the unsplit Zeeman multiplet. The trace over the operator (B9) vanishes unless $k=k'$, and we obtain

$$\mathrm{Tr}\sum_k C_{jk}^2 S_{zk}^2 = \tfrac{1}{3}S(S+1)\sum_k C_{jk}^2, \qquad (B10)$$

where S refers to the spin of the "other" species.

(2) We now evaluate the sum in (B10), using crystal parameters appropriate for ruby. Since the crystal symmetry greatly simplifies the explicit calculation, we refer angles to the crystal axis.

$$(3\cos^2\theta_{jk}-1)^2$$

$$= (4/5)+(8/7)P_2(\cos\theta_{jk})+(72/35)P_4(\cos\theta_{jk}) \qquad (B11)$$

$$= (4/5)+(32\pi/21)\sum_m Y_{2m}^*(\theta_H,\varphi_H)Y_{2m}(\theta_k,\varphi_k)$$

$$+ (32\pi/35)\sum_m Y_{4m}^*(\theta_H,\varphi_H)Y_{4m}(\theta_k,\varphi_k). \qquad (B12)$$

The threefold symmetry about the z axis leads to non-vanishing contributions only for m equal to an integral multiple of 3. Hence

$$\sum_k C_{jk}^2 = 12g_{Cr}^2 g_{Al}^2\beta^4/\hbar^2 \sum_i r_{ji}^{-6}$$

$$\times\{(1/5)+(10/21)P_{20}(\cos\theta_i)P_{20}(\cos\theta_H)$$

$$+ (18/35)P_{40}(\cos\theta_i)P_{40}(\cos\theta_H)+(1/4900)P_{43}(\cos\theta_i)$$

$$\times P_{43}(\cos\theta_H)\cos(3\varphi_{0i}-3\varphi_H)\}. \qquad (B13)$$

Here, i labels sets of equivalent atoms, that is, three atoms that go into each other under a $120°$ rotation about the z axis, and φ_{0i} is the angle of the projection of r_{ji} with the x axis. We define the x axis such that the next-nearest neighbor in the positive z direction has $r_x=0$.

The lattice constants[41,42] used were $a_{(hex)}=4.7664$ Å, $c=13.0146$ Å, nearest-neighbor distance$=2.73$ Å $=0.210c$. The sum was carried out over 342 atoms, or over a sphere of radius 4.5 times the nearest-neighbor distance. This guarantees an accuracy of at least 1%.

The result of the summation is (in cgs units):

$$\sum_k C_{jk}^2 = g_{Cr}^2 g_{Al}^2\beta^4/\hbar^2\times10^{45}$$

$$\times[16.42-19.60\cos^2\theta_H+18.70\cos^4\theta_H$$

$$-10.32\sin^3\theta_H\cos\theta_H\cos3\varphi_H]. \qquad (B14)$$

For $\theta_H=0$, this result reduces to 1.552×10^{46}.

To complete the calculation, we used the following constants:

$$g_{Cr}=1.9840, \quad g_{Al}=1.4563/1836,[43]$$

$$\partial f/\partial H = 2.80 \text{ Mc/sec/G}$$

for $0°$ orientation. We then obtain for the nuclear width

$$\text{rms width} = 4.36 \text{ Mc/sec} = 1.57 \text{ G.} \qquad (B15)$$

For a Gaussian line, half-width$=1.177\times$rms width; here

$$\text{half-width} = 5.12 \text{ Mc/sec} = 1.85 \text{ G.} \qquad (B16)$$

We note that Eq. (B14) predicts an angular dependence of the rms width, both in θ and in φ. Because of the small contribution of the nuclear dipole interaction to the total linewidth, it would be hopeless to observe this dependence. The Cr-Cr rms width is, of course, given by the same crystal sum. The angular dependence is not given correctly by (B14) in this case, however. Because of the zero-field terms of the Hamiltonian, which cannot now be ignored, a change in angle involves a change or a "mixing" of the energy levels. Such a change requires a different projection of S_x and a different truncation of the Hamiltonian. Even so, the appearance of φ in the formula at least raises the question whether a dependence on this angle could not actually exist.

APPENDIX C: ALUMINUM NUCLEAR MAGNETIC RESONANCE LINE SHAPE

Our main object in this Appendix is to clarify the question of analogy arguments in the context of line shapes, and to indicate the relative effect of self-

[41] G. Shinoda and Y. Amano, X-Rays (Japan) 6, 7 (1950).
[42] R. W. G. Wyckoff, *Crystal Structures* (Interscience Publishers, Inc., New York, 1957), Vol. 2, Chap. 5, pp. 4, 13b.
[43] N. F. Ramsay, *Nuclear Moments* (John Wiley & Sons, Inc., New York, 1953), Chap. 4.

broadening and Cr broadening on the aluminum nuclear magnetic resonance width.

The Al-Al broadening cannot be derived from the Cr-Cr broadening. For Al, the concentration is almost 1, and the self-broadened line will be close to Gaussian; for Cr, the small concentration produces a Lorentz line. The two line shapes have completely different properties, as we have taken pains to stress. Thus, there is no easy theoretical bridge between observed line shapes of the Cr resonance and observed line shapes of the Al resonance.

On the other hand, a straightforward second moment calculation will describe the Al-Al width to a reasonable approximation. The result will differ from the second moment of the Cr-Cr interaction, because of the different g factors and spins, and because of numerical coefficients arising from projecting the transition out of a different manifold. For Cr, the ratio of the projected moment to the simple Zeeman multiplet moment is 0.9. We shall not worry about errors of the order of 10% here, and calculate without projection operators. Using the crystal sum (33), we obtain for the full rms linewidth of the self-broadened nuclear resonance 1.85 kc/sec.

The broadening effect of Cr on Al, again, has no analogy to the broadening effect of Al on Cr. Paradoxical as this statement sounds, it is nonetheless true, because of the incommensurability of the line shapes derived from these interactions. The effect of Cr on Al is analogous to the effect of Cr on Cr, in the sense that both give rise to Lorentz shapes, differing principally by scale factors. The difference is not only in the g factors, of course. We again have the problem of projecting transitions from different manifolds, and the problem that one case is heterogeneous broadening while the other is self-broadening. We shall again ignore the first difficulty, and approximate the second by the well-known $\frac{2}{3}$ factor. From our calculation of Cr-Cr broadening, discussed in Sec. IV, if we take $r_0 = 2.73$ Å (the nearest-neighbor distance), we obtain in the limit of vanishing concentrations,

$$\text{peak-peak derivative width} = 2.1 \times 10^4 \text{ n Mc/sec.} \quad \text{(C1)}$$

After making the appropriate corrections, this number becomes, for the Cr-Al effect,

$$\text{peak-peak derivative width} = 0.9 \times 10^4 \text{ n kc/sec.} \quad \text{(C2)}$$

The Al nuclear resonance has been measured by Pound[44] and by Strandberg[45]: Pound observes a p-p width of 4 kc/sec; Strandberg observes a p-p width of 8.7 kc/sec. Pound's number is insignificantly larger than the 3.7 kc/sec we calculate on a pure Al-Al basis. Strandberg's could be interpreted in terms of a 0.085% Cr concentration.

[44] R. V. Pound, Phys. Rev. **79**, 685 (1950).
[45] M. W. P. Strandberg, Tenth Quarterly Progress Report, Signal Corps Contract DA36-039-sc-74895, Research Laboratory of Electronics, MIT, Cambridge, Massachusetts, 15 February 1960 (unpublished).